



PERGAMON

Available online at www.sciencedirect.com

SCIENCE @ DIRECT®

Computers
& Structures

Computers and Structures 81 (2003) 287–298

www.elsevier.com/locate/comprstruc

Focussed adaptivity for laminated plates

P.M. Mohite, C.S. Upadhyay *

Department of Aerospace Engineering, Indian Institute of Technology, Kanpur 208016, India

Received 30 January 2002; accepted 2 November 2002

Abstract

Accurate computation of the critical response quantities for laminated composite structures has become essential, especially from the design and design certification point of view. Worst case scenario analysis (corresponding to the load envelope) of the structure require computation of local quantities of interest. In such a situation, control of both modelling error and discretisation error for the quantities of interest is required.

In this study, for a fixed plate model, a novel adaptive procedure is presented, based on a posteriori estimation of the error in the quantity of interest. This focussed adaptive procedure involves prediction of the desired optimal mesh sizes in the neighborhood of the region of interest and away from the region of interest, based on an a priori estimate of the error in the quantity of interest. The final desired mesh is obtained in one shot. It is found that the error estimator, for the quantity of interest is reasonably robust. Further, the adaptive procedure is very effective in controlling the local error to within the specified tolerances.

© 2003 Elsevier Science Ltd. All rights reserved.

1. Introduction

Composites are increasingly employed in the manufacture of lightweight components. Thin plate or shell type members are often used in aircraft wing, fuselage or auxillary devices. The inherent heterogeneity in the material properties makes the analysis and design of these components more challenging.

Often, in the analysis or design of laminated structures the critical quantities have to be evaluated accurately, for the given load envelope. The critical quantities of interest are maximum stress, deflection, buckling load, first ply failure load, etc. Shape and topology optimization procedures employ these critical quantities as constraint data (see [1] for example). Obviously, accurate evaluation of the critical data is essential for the success of the optimization procedure.

Adaptive methods are available in the literature (see [9–11]), for the control of the discretisation error. Often, these are based on the control of the energy norm of the error, $\|\mathbf{e}\|_{\Omega}$ which is given by $\|\mathbf{e}\|_{\Omega} = \sqrt{2\mathcal{U}(\mathbf{e})}$ (where $\mathcal{U}(\mathbf{e})$ is the strain energy of the error). This does not guarantee that the particular data of interest is also accurate (i.e. error is within desired tolerances). Often, critical stress or strain data can have significant error eventhough the energy norm is within acceptable tolerances.

In [6,8] it was shown that the error in the quantity of interest can be given in terms of error in the solution of an auxillary problem. The focus of [5,6] was to control the “pollution” error in the quantity of interest.

The goal of the current study is to develop a simple procedure for the estimation and adaptive control of the error in the quantities of interest. The aim is to construct a “one-shot” adaptive approach for the control of the discretisation error, for laminated plates. The important issue of control of modelling error (i.e. error in the plate model as compared to three dimensional elasticity) will not be discussed here. Simultaneous control of modelling as well as discretisation error will be the subject of a subsequent paper.

* Corresponding author.

E-mail address: shekhar@iitk.ac.in (C.S. Upadhyay).

2. Plate formulation

Several plate models are available in the literature (see [2,3]). For the laminated plates, we employ the model given in [2]. For this model, we have

$$\mathbf{u}(x, y, z) = \begin{Bmatrix} u(x, y, z) \\ v(x, y, z) \\ w(x, y, z) \end{Bmatrix} = [\phi(z)]\mathbf{U}(x, y) \tag{1}$$

where

$$[\phi(z)] = \begin{bmatrix} \phi_1(z) & 0 & \phi_3(z) & 0 & 0 & \phi_6(z) & 0 & 0 & \phi_9 & 0 & 0 & \dots \\ 0 & \phi_2(z) & 0 & \phi_4(z) & 0 & 0 & \phi_7(z) & 0 & 0 & 0 & \phi_{10}(z) & \dots \\ 0 & 0 & 0 & 0 & \phi_5(z) & 0 & 0 & \phi_8(z) & 0 & 0 & \phi_{11}(z) & \dots \end{bmatrix} \tag{2}$$

and

$$\mathbf{U} = \{ U_1(x, y) \quad U_2(x, y) \quad U_3(x, y) \quad \dots \quad U_{11}(x, y) \quad \dots \}^T \tag{3}$$

Note that $U_1(x, y), U_3(x, y), U_6(x, y), U_{11}(x, y), \dots$ are the in-plane components of the displacement term $u(x, y, z)$. Similarly, $U_2(x, y), U_4(x, y), U_7(x, y), U_{10}(x, y), \dots$ are the in-plane components for the displacement term $v(x, y, z)$. The in-plane components of the transverse displacement $w(x, y, z)$ are given by $U_5(x, y), U_8(x, y), U_{11}(x, y), \dots$. In this study only the first eight terms in the expansion will be used (i.e. eight-field model), for which the transverse functions are given in terms of the normalized transverse coordinate $\hat{z} = (2/t)z$ (where t is the thickness of the laminate), as (see [2] for details)

$$\begin{aligned} \phi_1(\hat{z}) &= \phi_2(\hat{z}) = \phi_5(\hat{z}) = 1, & \phi_3(\hat{z}) &= \phi_4(\hat{z}) = \hat{z} \frac{t}{2} \\ \phi_6(\hat{z}) &= \frac{t}{2} \{ \varphi(\hat{z}) - \varphi(0) \}, & \phi_7(\hat{z}) &= \frac{t}{2} \{ \psi(\hat{z}) - \psi(0) \} \\ \phi_8(\hat{z}) &= \frac{t}{2} \{ \rho(\hat{z}) - \rho(0) \} \end{aligned}$$

where

$$\begin{aligned} \varphi(\hat{z}) &= \int_{-1}^{\hat{z}} \frac{Q_{44} - Q_{45}}{Q_{44}Q_{55} - Q_{45}^2} d\hat{z}; \\ \psi(\hat{z}) &= \int_{-1}^{\hat{z}} \frac{Q_{55} - Q_{45}}{Q_{44}Q_{55} - Q_{45}^2} d\hat{z}; & \rho(\hat{z}) &= \int_{-1}^{\hat{z}} \frac{1}{Q_{33}} d\hat{z} \end{aligned}$$

where Q_{ij} are the coefficients of the global constitutive relation, in the global xyz -coordinate system.

For a given lamina l the constitutive relationship, in the principal material directions is given as

$$\{\bar{\sigma}^{(l)}\} = [C^{(l)}]\{\bar{\epsilon}^{(l)}\} \tag{4}$$

where $\{\bar{\sigma}^{(l)}\} = \{\sigma_{11}^{(l)} \quad \sigma_{22}^{(l)} \quad \sigma_{33}^{(l)} \quad \sigma_{23}^{(l)} \quad \sigma_{13}^{(l)} \quad \sigma_{12}^{(l)}\}^T$ are the stress components for the layer, and $\{\bar{\epsilon}^{(l)}\} = \{\epsilon_{11}^{(l)} \quad \epsilon_{22}^{(l)} \quad \epsilon_{33}^{(l)} \quad \gamma_{23}^{(l)} \quad \gamma_{13}^{(l)} \quad \gamma_{12}^{(l)}\}^T$ are the strain components for the layer. Note that here the subscripts 1, 2, 3 corre-

spond to the three principal material directions. The constitutive relationship in the global xyz -coordinates (for each lamina) can be obtained by the usual transformation to get

$$\{\sigma^{(l)}\} = [Q^{(l)}]\{\epsilon^{(l)}\} \tag{5}$$

with $\{\sigma^{(l)}\} = \{\sigma_{xx}^{(l)} \quad \sigma_{yy}^{(l)} \quad \sigma_{zz}^{(l)} \quad \sigma_{yz}^{(l)} \quad \sigma_{xz}^{(l)} \quad \sigma_{xy}^{(l)}\}^T$ and the strain $\{\epsilon^{(l)}\} = \{\epsilon_{xx} \quad \epsilon_{yy} \quad \epsilon_{zz} \quad \gamma_{yz} \quad \gamma_{xz} \quad \gamma_{xy}\}^T$, and $[Q^{(l)}]$ can be obtained from $[C^{(l)}]$ by transformation from the principal material coordinates to the global xyz -coordinates.

The potential energy, Π , for the structure is given by

$$\Pi = \frac{1}{2} \int_V \{\sigma\} \cdot \{\epsilon\} dV - \int_{R^+ \cup R^-} q w ds \tag{6}$$

where V is the volume enclosed by the plate domain, R^+ and R^- are the top and bottom faces of the plate and $q(x, y)$ is the applied transverse load on these faces (see Fig. 1).

The solution to the problem, \mathbf{u}_{ex} , is the minimizer of the total potential Π , and is given as

Find $\mathbf{u}_{ex} \in \mathbf{H}^0(V)$ such that

$$B(\mathbf{u}_{ex}, \mathbf{v}) = F(\mathbf{v}) \quad \forall \mathbf{v} \in \mathbf{H}^0(V) \tag{7}$$

where $\mathbf{H}^0(V) = \{\mathbf{u} = [\Phi]\mathbf{U} | \mathcal{W}(\mathbf{u}) < \infty \text{ and } [\mathbf{M}]\mathbf{U} = \mathbf{0} \text{ on } \Gamma_D\}$. Here $\Gamma = \Gamma_N \cup \Gamma_D$ is the lateral boundary of the plate with the Dirichlet part Γ_D and Neumann part Γ_N . Note that in this study Dirichlet means the parts of the lateral boundary where geometric constraints are imposed, while Neumann stands for the stress-free parts of the lateral boundary. Further, $[\mathbf{M}]$ depends on the type of Dirichlet condition on the edge, i.e. clamped; soft simple-support; hard simple-support etc.

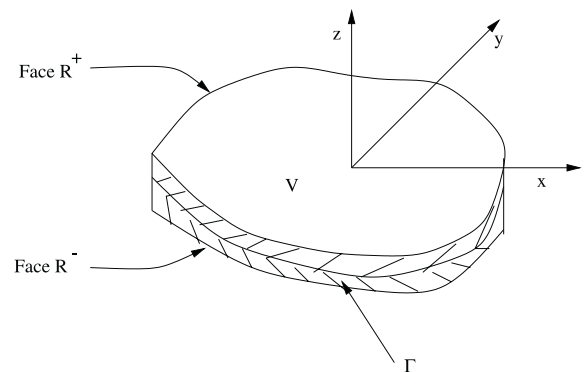


Fig. 1. A laminated plate with top and bottom surfaces R^+ and R^- .

Hence, we have

$$B(\mathbf{u}_{\text{ex}}, \mathbf{v}) = \sum_l B_l(\mathbf{u}_{\text{ex}}, \mathbf{v}) = \sum_l \int_{V_l} \{\sigma_{(l)}(\mathbf{u}_{\text{ex}})\} \cdot \{\epsilon_{(l)}(\mathbf{v})\} dV$$

and

$$F(\mathbf{v}) = \int_{R^+ \cup R^-} qv_3 ds \tag{8}$$

where V_l is the volume of the l^{th} lamina in the laminate; v_3 is the transverse component of the test function \mathbf{v} .

3. Definition of error estimator

The variational formulation (8) is used to obtain the finite element solution $\mathbf{u}_h \in \mathbf{H}_h^0(V)$, where $\mathbf{H}_h^0(V) = \{\mathbf{u} = [\Phi]\mathbf{U}; U_i \in S_p^e, i = 1, 2, 3, \dots | \mathcal{W}(\mathbf{u}) < \infty, [\mathbf{M}]\mathbf{U} = \mathbf{0} \text{ on } \Gamma_D\}$. Letting ω_{2D} be the plate mid surface with boundary $\partial\omega_{2D}$, we define S_τ^p as the set of globally continuous piecewise polynomials of order p over each element τ ($\tau \in \omega_{2D}$). Thus, we have

$$B(\mathbf{u}_h, \mathbf{v}_h) = F(\mathbf{v}_h) \quad \forall \mathbf{v}_h \in \mathbf{H}_h^0(V) \tag{9}$$

Note that $\mathbf{u}_h = [\phi]\mathbf{U}_h$ is the representation of \mathbf{u}_h , following (1). The error in the solution can be given as $\mathbf{e} = \mathbf{u}_{\text{ex}} - \mathbf{u}_h$. An approximation to the error can be given as $\mathbf{e}^* = \mathbf{u}^* - \mathbf{u}_h$ where $\mathbf{u}^* \in S_\tau^{p+k}$ is obtained for each element τ as described below (see [4] for details). In all the numerical examples $k = 2$ has been employed.

For an element τ let P_τ be the patch of elements in a one-layer neighborhood of τ , as shown in Fig. 2.

Over the patch P_τ , define

$$\mathbf{u}^* = \begin{Bmatrix} u^* \\ v^* \\ w^* \end{Bmatrix} = [\phi]\mathbf{U}^*$$

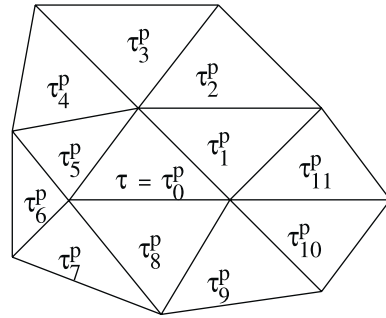


Fig. 2. Element τ with the patch P_τ consisting of elements $\{\tau_i^{(p)}\}_{i=0,1,\dots,11}$.

where

$$U_i^* = \sum_{j=1}^{\text{NDOF}} A_{ij} q_j(x, y)$$

with $\text{NDOF} = (p + 1 + k)(p + 2 + k)/2$; $q_j(x, y)$ as the monomials of order $\leq p + k$ (see [4] for details) defined in terms of the local coordinates $\hat{x} = x - x_c^e, \hat{y} = y - y_c^e$. Here x_c^e, y_c^e are the centroidal coordinates for the element τ . The $q_j(x, y)$ can be given as

$$\begin{aligned} q_1(x, y) &= 1, & q_2(x, y) &= \hat{x}, & q_3(x, y) &= \hat{y}, \\ q_4(x, y) &= \hat{x}^2, & q_5(x, y) &= \hat{x}\hat{y}, & q_6(x, y) &= \hat{y}^2, \dots \end{aligned} \tag{10}$$

The coefficients A_{ij} are obtained by minimizing $J = \frac{1}{2} \int_{A_{P_\tau}} |\mathbf{U}^* - \mathbf{U}_h|^2 dA$ where A_{P_τ} is the area of the patch P_τ (where $A_{P_\tau} \subset \omega_{2D}$). This definition is called the L_2 projection based error estimator (see [4] for details).

4. The auxillary problem

Let us consider the domain of Fig. 3. Let us further assume that we are interested in the value of stress

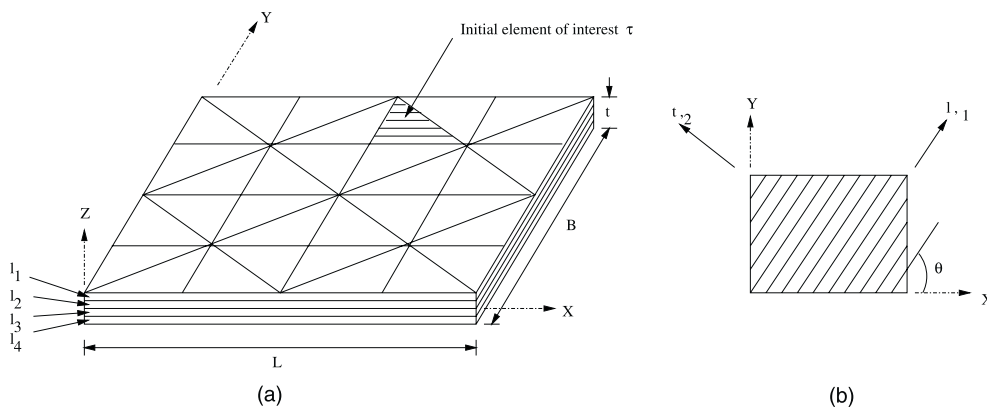


Fig. 3. (a) Laminated plate with initial mesh T and element of interest τ . (b) Lamina with material coordinates l, t (or 1, 2).

component σ_{xx} in the topmost layer, for all points in the element τ (shown shaded in Fig. 3).

In order to accurately obtain the pointwise information in τ , we will let $\sigma_{xx,avg}^{(l)} = \frac{1}{v_\tau^l} \int_{v_\tau^l} \sigma_{xx} dv$ as the quantity of interest. Here $v_\tau^l = A_\tau t_l$ is the volume enclosed by the element τ in the l^{th} layer. Hence,

$$\sigma_{xx,avg}^{(l)} = \frac{1}{A_\tau t_l} \int_{z=z_{l-1}}^{z_l} \int_{A_\tau} (\sigma_{xx} dA) dz \tag{11}$$

with t_l as the thickness of the l^{th} layer; z_{l-1} and z_l as the lower and upper z coordinate for the l^{th} layer; A_τ is the area of element τ .

Remark. Using the average stress in an element, as the quantity of interest, is allowable. This is because control of error in the average stress will ensure accurate values of the pointwise stresses, for all points in the element τ . Further, taking the average over the layer ensures that the stress at all points within the layer will be accurately obtained. We could have taken a slice of the layer (in the vicinity of the interface, for example), as the volume of interest.

Corresponding to $\sigma_{xx,avg}^{(l)}$ we define the following auxillary problem:

Find $\mathbf{G} \in \mathbf{H}^0(V)$ such that

$$B(\mathbf{G}, \mathbf{v}) = \sigma_{xx,avg}^{(l)}(\mathbf{v}) = \mathcal{F}(\mathbf{v}) \quad \forall \mathbf{v} \in \mathbf{H}^0(V) \tag{12}$$

Letting $\mathbf{G}_h \in \mathbf{H}_h^0(V)$ be the finite element solution for \mathbf{G} , we have

$$B(\mathbf{G}_h, \mathbf{v}_h) = \sigma_{xx,avg}^{(l)}(\mathbf{v}_h) = \mathcal{F}(\mathbf{v}_h) \quad \forall \mathbf{v}_h \in \mathbf{H}_h^0(V) \tag{13}$$

Note that letting the approximation for \mathbf{G} to be of the same order, p , as \mathbf{u}_h , the auxillary problem gives rise to an additional load vector. Hence, any direct solver, with capability to handle multiple load vectors, can be employed to solve for \mathbf{u}_h and \mathbf{G}_h simultaneously. Further, it should be noted that the same procedure can be carried out for any stress component σ_i , or strain component ϵ_i , displacement \mathbf{u} etc. Simultaneously, all the desired components can be solved for without increasing the computational cost significantly.

5. Estimators for error in quantity of interest

From the previous section we have

$$B(\mathbf{G}, \mathbf{u}_{ex} - \mathbf{u}_h) = \mathcal{F}(\mathbf{u}_{ex}) - \mathcal{F}(\mathbf{u}_h) = \mathcal{F}(\mathbf{u}_{ex} - \mathbf{u}_h) = \mathcal{F}(\mathbf{e}) \tag{14}$$

From the orthogonality property of the error in the finite element solution, we have

$$|B(\mathbf{G} - \mathbf{G}_h, \mathbf{u}_{ex} - \mathbf{u}_h)| = |\mathcal{F}(\mathbf{e})| \tag{15}$$

or

$$\begin{aligned} |\mathcal{F}(\mathbf{e})| &= |B(\mathbf{G} - \mathbf{G}_h, \mathbf{u}_{ex} - \mathbf{u}_h)| \\ &\leq \sum_{\tau} |B(\mathbf{G} - \mathbf{G}_h, \mathbf{u}_{ex} - \mathbf{u}_h)| \\ &\leq \sum_{\tau} \|\mathbf{e}_u\|_{\tau} \|\mathbf{e}_G\|_{\tau} \leq \|\mathbf{e}_u\| \|\mathbf{e}_G\| \end{aligned} \tag{16}$$

where $\mathbf{e}_u = \mathbf{e}$ stands for the error in the actual solution and \mathbf{e}_G stands for the error in the auxillary problem. Thus, we can see that the smoothness of both \mathbf{u} and \mathbf{G} affect the measure of error in the quantity of interest.

6. Definition of a posteriori error estimators for local quantity of interest

Replacing \mathbf{e}_u with the estimate \mathbf{e}_u^* and \mathbf{e}_G with the estimate \mathbf{e}_G^* , we can get the following definitions of the estimators, for the error in the quantity of interest:

(1) Estimator 1 (E_1)

$$|\mathcal{F}(\mathbf{e})|_{E_1} = \left| \sum_{\tau} B(\mathbf{e}_u^*, \mathbf{e}_G^*) \right| \tag{17}$$

(2) Estimator 2 (E_2)

$$|\mathcal{F}(\mathbf{e})|_{E_2} = \sum_{\tau} |B(\mathbf{e}_u^*, \mathbf{e}_G^*)| \tag{18}$$

(3) Estimator 3 (E_3)

$$|\mathcal{F}(\mathbf{e})|_{E_3} = \sum_{\tau} \|\mathbf{e}_u^*\| \|\mathbf{e}_G^*\| \tag{19}$$

Remark. Estimators E_2 and E_3 will be more conservative, as compared to E_1 . Note that in the definition E_1 , the signs of the elemental contributions to the total error can be different, leading to cancellations. However, from the error estimation and adaptivity point of view, we would like to control the intensity (or magnitude) of the elemental contributions to the error in the quantity of interest. This will ensure a uniform decrease in the pointwise errors at a point, or in an element.

In the numerical results given below, we study the quality of the a posteriori error estimates for the quantity of interest (or focussed error estimators) for various ply orientations and boundary conditions.

7. Numerical study of the quality of a posteriori error estimators

The quality of the error estimator, for the quantity of interest, has to be ascertained. In this study we will use the L_2 projection based estimators \mathbf{e}_u^* and \mathbf{e}_G^* (given by definitions (9) and (10)). For this choice of the a poste-

riori error estimator we have to determine the quality of the three definitions of the focussed error estimators E_1 , E_2 and E_3 .

In order to study the reliability of the error estimators, we let $\mathbf{u}_h^{(p)}$, $\mathbf{G}_h^{(p)}$ be the finite element solutions of the order p for \mathbf{u}_{ex} and \mathbf{G} . Thus, we can approximate error \mathbf{e}_u as $\mathbf{e}_u \approx \mathbf{e}_u^{(p+1)} = \mathbf{u}_h^{(p+1)} - \mathbf{u}_h^{(p)}$ and hence $\mathcal{F}(\mathbf{e}) \approx \mathcal{F}(\mathbf{e}_u^{(p+1)})$. It can be shown that $\mathcal{F}(\mathbf{e}_u^{(p+1)}) = \sum_{\tau} B(\mathbf{e}_G^{(p+1)}, \mathbf{e}_u^{(p+1)})$. With this definition of the “exact” error, we let the effectivity index for the quantity of interest $\kappa_{\mathcal{F}}$ be defined as

$$\kappa_{\mathcal{F}} = \frac{|\mathcal{F}(\mathbf{e}^*)|_{E_i}}{|\mathcal{F}(\mathbf{e})|_{E_i}} \quad i = 1, 2, 3 \tag{20}$$

Letting τ be the element of interest and P the one-layer neighborhood of τ , the total error can be partitioned into two parts as follows:

$$|\mathcal{F}(\mathbf{e})| \leq |\mathcal{F}_1(\mathbf{e})| + |\mathcal{F}_2(\mathbf{e})|$$

where

$$\mathcal{F}_1(\mathbf{e}) = \sum_{\tau \in P} B(\mathbf{e}_u, \mathbf{e}_G), \quad \mathcal{F}_2(\mathbf{e}) = \sum_{\tau \in P'} B(\mathbf{e}_u, \mathbf{e}_G) \tag{21}$$

where P' is the set of elements lying outside P . Following [6], $\mathcal{F}_1(\mathbf{e})$ is the local part of the error and $\mathcal{F}_2(\mathbf{e})$ is the “pollution” in the quantity of interest (i.e. far-field influence). For each of these quantities, we can obtain the effectivity indices $\kappa_{\mathcal{F}_1}$ and $\kappa_{\mathcal{F}_2}$, by suitably modifying definition (20).

Remark. The significant part of the true error can be given in terms of the $(p + 1)$ part of the error, when the pollution (or far-field influence) is not significant (see [7]). The far-field effect is significant when reentrant corners are present in the domain.

Remark. Note that \mathbf{G} is badly behaved in P . Hence, \mathbf{e}_G does not converge locally. Thus, in P , \mathbf{e}_G is not approximated well by $\mathbf{e}_G^{(p+1)}$. This means that in P , \mathbf{e}_G^* (or

the estimated error) is not a reliable estimate of \mathbf{e}_G . However, in the numerical procedure we employ \mathbf{e}_G^* instead of \mathbf{e}_G . It will be observed, in the numerical examples that the estimator is still reasonably robust.

We consider the following rectangular laminated plate configuration:

- length $L = 10$ cm; breadth $B = 10$ cm;
- thickness $t = 1$ cm (moderately thick plate) or $t = 1$ mm (thin plate);
- number of lamina, NLAY = 4 (of equal thickness);
- $E_{11} = 138$ MPa; $E_{tt} = 9.3$ MPa; $\nu_{lt} = 0.3$; $\nu_{tt} = 0.5$;
- $G_{lt} = 4.6$ MPa; $G_{tt} = 3.1$ MPa;
- loading: uniformly distributed transverse loading on R^+ , $q(x, y) = 100$ kPa.

Here l denotes the fibre direction, for a lamina, and t denotes the transverse direction (see Fig. 3).

For the plate configuration we consider the following boundary conditions:

- clamped–clamped (CCCC): for $x = 0, L$; $y = 0, B$; $u = v = w = 0$,
- clamped–free (CFCF): for $x = 0, L$; $u = v = w = 0$,
- simply-supported (SSSS): for $x = 0, L$; $v = w = 0$; for $y = 0, B$; $u = w = 0$.

Laminates with material orientation of $[0/90/90/0]$ and $[-45/45/45/-45]$ were considered in the numerical examples. Further, it should be noted that in all the examples, the stress quantities have units of kPa. Quadratic finite element approximations ($p = 2$) are employed throughout this study. The order of approximation, p , will be specifically mentioned wherever p other than 2 is employed.

In Tables 1 and 2 we report the value of $\mathcal{K}_{\mathcal{F}}$ (for total error) and $\mathcal{K}_{\mathcal{F}_2}$ (for pollution error) for a thin plate. We observe that

Table 1
Quality of estimator for $[0/90/90/0]$; plate dimension: $10 \times 10 \times 0.1$

Quantity	BC	$\kappa_{\mathcal{F}}$			$\kappa_{\mathcal{F}_2}$			% error
		E_1	E_2	E_3	E_1	E_2	E_3	
$\sigma_{xx,avg}^{(1)} = -96.05$	CCCC	0.92	0.87	1.42	0.08	0.65	1.04	51.00
$\sigma_{xx,avg}^{(1)} = -2038.78$	CFCF	0.85	0.91	1.34	1.02	1.18	1.17	02.00
$\sigma_{xx,avg}^{(1)} = -1930.34$	SSSS	0.16	1.07	1.75	1.57	1.38	1.39	21.00
$\sigma_{yy,avg}^{(1)} = 230.97$	CCCC	1.55	0.82	1.10	1.78	1.66	1.33	16.00
$\sigma_{yy,avg}^{(1)} = -63.71$	CFCF	1.83	1.35	1.31	1.48	1.39	1.33	10.00
$\sigma_{yy,avg}^{(1)} = -304.66$	SSSS	0.47	0.83	1.39	5.22	1.26	1.41	09.00
$\sigma_{xy,avg}^{(1)} = 113.17$	CCCC	1.43	0.80	1.11	1.61	1.47	1.35	17.00
$\sigma_{xy,avg}^{(1)} = -73.46$	CFCF	2.17	1.22	1.31	1.58	1.39	1.34	0.003
$\sigma_{xy,avg}^{(1)} = -191.74$	SSSS	0.35	0.84	1.33	8.09	1.20	1.43	11.00

Table 2
Quality of estimator for $[-45/45/45/-45]$; plate dimension: $10 \times 10 \times 0.1$

Quantity	BC	$\kappa_{\mathcal{F}}$			% error
		E_1	E_2	E_3	
$\sigma_{xx,avg}^{(1)} = -1880.40$	SSSS	1.52	0.93	1.37	01.500
$\sigma_{yy,avg}^{(1)} = -119.18$	SSSS	0.06	0.69	1.17	79.400
$\sigma_{xy,avg}^{(1)} = -97.99$	SSSS	0.08	0.73	1.19	47.700
$\sigma_{xx,avg}^{(1)} = 1020.91$	CCCC	0.71	0.68	1.18	25.800
$\sigma_{yy,avg}^{(1)} = 189.55$	CCCC	45.43	0.87	1.04	05.000
$\sigma_{xy,avg}^{(1)} = 115.04$	CCCC	5.24	0.85	1.08	04.200
$\sigma_{xx,avg}^{(1)} = -994.24$	CFCF	3.39	1.15	1.34	12.700
$\sigma_{yy,avg}^{(1)} = -313.20$	CFCF	0.28	0.55	1.09	32.900
$\sigma_{xy,avg}^{(1)} = -176.08$	CFCF	0.46	0.56	1.13	27.900

- (1) Estimator E_1 is not reliable.
- (2) Estimator E_3 is very robust ($1.04 \leq \kappa_{\mathcal{F}} \leq 2.05$), but estimator E_2 can underestimate the error (especially for the $[-45/45/45/-45]$ laminate), with $\kappa_{\mathcal{F}} \geq 0.55$.
- (3) Estimator E_1 is sensitive to the boundary condition. For example, for SSSS underestimation is severe. However, E_2 and E_3 are insensitive to the boundary-condition type.
- (4) In the region P' , E_1 is completely unreliable with $0.06 \leq \kappa_{\mathcal{F}_2} \leq 46.0$. Estimators E_2 and E_3 are robust in P' .
- (5) The error in the quantity of interest can be very high ($>50\%$), for the mesh shown in Fig. 3.

For the moderately thick plate (see Table 3), we note that the error in the quantity of interest is small. Further, as observed above for the thin plate, estimator E_1 is unreliable while E_2 and E_3 are robust.

Remark. Estimator E_1 cannot be guaranteed to be reliable because $B(\mathbf{e}_u^*, \mathbf{e}_G^*)$ need not be of the same sign as $B(\mathbf{e}_u, \mathbf{e}_G)$ in each element of the current mesh. Thus, cancellation of error contributions from each element will not be properly accounted for by the estimator. This can result in discrepancies in the estimated error. Estimator E_2 is more reliable because the sign of $B(\mathbf{e}_u, \mathbf{e}_G)$ is not important in its definition.

Table 3
Quality of estimator for $[0/90/90/0]$; plate dimension: $10 \times 10 \times 1$

Quantity	BC	$\kappa_{\mathcal{F}}$			$\kappa_{\mathcal{F}_2}$			% error
		E_1	E_2	E_3	E_1	E_2	E_3	
$\sigma_{xx,avg}^{(1)} = -2.26$	CCCC	3.52	1.47	2.04	0.04	0.72	1.17	1.000
$\sigma_{xx,avg}^{(1)} = -20.71$	CFCF	30.69	1.07	1.75	0.59	0.74	1.18	0.003
$\sigma_{xx,avg}^{(1)} = -14.87$	SSSS	1.04	1.25	2.07	13.85	1.14	1.33	0.300
$\sigma_{yy,avg}^{(1)} = 2.76$	CCCC	1.02	1.22	1.99	0.98	1.05	1.72	2.000
$\sigma_{yy,avg}^{(1)} = -0.71$	CFCF	0.04	1.28	2.01	0.61	1.54	1.95	0.800
$\sigma_{yy,avg}^{(1)} = -3.34$	SSSS	0.26	1.17	2.05	6.09	1.05	2.06	0.800
$\sigma_{xy,avg}^{(1)} = 0.97$	CCCC	1.08	1.46	1.36	0.72	0.89	1.90	2.000
$\sigma_{xy,avg}^{(1)} = -1.16$	CFCF	0.13	1.41	1.59	0.51	1.36	1.85	0.300
$\sigma_{xy,avg}^{(1)} = -2.34$	SSSS	0.05	1.23	1.55	12.49	1.21	2.05	0.700

Remark. Estimators E_2 and E_3 do a reasonable job of predicting the pollution error. Eventhough \mathbf{e}_G^* will not be reliable in region P , we find that the estimate (i.e. using $\mathcal{F}(\mathbf{e})$) is reasonably robust.

Since $|\mathcal{F}(\mathbf{e})|_{E_1} \leq |\mathcal{F}(\mathbf{e})|_{E_2} \leq |\mathcal{F}(\mathbf{e})|_{E_3}$, it is important to find out how severe the over-estimation of the error can be when definition E_2 and E_3 are employed. In Tables 4 and 5 we report the ratios $\mathcal{R}_1 = |\mathcal{F}(\mathbf{e})|_{E_2} / |\mathcal{F}(\mathbf{e})|_{E_1}$ and $\mathcal{R}_2 = |\mathcal{F}_2(\mathbf{e})|_{E_2} / |\mathcal{F}_2(\mathbf{e})|_{E_1}$, for the thin and thick plate with $[0/90/90/0]$ stacking sequence. From Tables 4 and 5 we observe that

- 1. For the thin plate, where the error is significant, over-estimation due to definition E_2 of the error, is moderate with $\mathcal{R}_1 \leq 6$.
- 2. For the thick plate also, in general, over-estimation is moderate. For the case when $\mathcal{R}_1 \approx 150$, the actual error is very small ($<0.003\%$). Thus, the over-estimated error also turns out to be very small.
- 3. The over-estimation depends on the plate thickness and boundary-condition type.
- 4. In region P' , the over-estimation can be severe ($\mathcal{R}_2 > 15$ can be observed).

It should be noted that Tables 4 and 5 correspond to ratios of quantities computed using the “exact” errors.

Table 4
Over-estimation (definition E_2) for [0/90/90/0]; plate dimension: $10 \times 10 \times 0.1$

Quantity	BC	\mathcal{R}_1	\mathcal{R}_2
$\sigma_{xx,avg}^{(1)} = -96.05$	CCCC	5.85	1.42
$\sigma_{xx,avg}^{(1)} = -2038.78$	CFCF	1.82	3.07
$\sigma_{xx,avg}^{(1)} = -1930.34$	SSSS	1.65	8.66
$\sigma_{yy,avg}^{(1)} = 230.97$	CCCC	1.92	1.95
$\sigma_{yy,avg}^{(1)} = -63.71$	CFCF	2.75	2.78
$\sigma_{yy,avg}^{(1)} = -304.66$	SSSS	3.23	17.28
$\sigma_{xy,avg}^{(1)} = 113.17$	CCCC	1.88	1.75
$\sigma_{xy,avg}^{(1)} = -73.46$	CFCF	4.04	3.71
$\sigma_{xy,avg}^{(1)} = -191.74$	SSSS	2.34	32.02

Table 5
Over-estimation (definition E_2) for [0/90/90/0]; plate dimension: $10 \times 10 \times 1$

Quantity	BC	\mathcal{R}_1	\mathcal{R}_2
$\sigma_{xx,avg}^{(1)} = -2.26$	CCCC	9.49	1.24
$\sigma_{xx,avg}^{(1)} = -20.71$	CFCF	149.35	18.54
$\sigma_{xx,avg}^{(1)} = -14.87$	SSSS	6.27	207.46
$\sigma_{yy,avg}^{(1)} = 2.76$	CCCC	1.72	1.81
$\sigma_{yy,avg}^{(1)} = -0.71$	CFCF	2.17	8.84
$\sigma_{yy,avg}^{(1)} = -3.34$	SSSS	2.44	14.19
$\sigma_{xy,avg}^{(1)} = 0.97$	CCCC	2.23	1.28
$\sigma_{xy,avg}^{(1)} = -1.16$	CFCF	2.54	7.52
$\sigma_{xy,avg}^{(1)} = -2.34$	SSSS	2.47	31.97

From the result we note that the over-estimation for the total error, as well as pollution, can be significant when definition E_2 is employed. However, since the goal of the adaptive process (to be discussed below) is to uniformly control the intensity of the contribution (from various elements) to the quantity of interest, definitions E_2 and E_3 are appropriate measures of the error.

8. One-shot adaptivity for quantity of interest

In the previous section we presented the a posteriori error estimators for the quantity of interest. Here, we will give an adaptive procedure by which the desired optimal mesh can be obtained from an initial mesh computation directly. It will be shown in the subsequent section that the desired optimal mesh indeed leads to reduction of the error within specified tolerances.

Following [5], we can partition the contribution to the total error, $\mathcal{F}(\mathbf{e})$, into two parts $\mathcal{F}(\mathbf{e}) = \mathcal{F}_1(\mathbf{e}) + \mathcal{F}_2(\mathbf{e})$, as defined by (21). Following [8], we observe that the auxillary function \mathbf{G} is unsmooth in P hence

$$|\mathcal{F}_1(\mathbf{e})| \leq \sum_{\tau \in P} \|\mathbf{e}_\tau\| \|\mathbf{e}_\mathbf{G}\| \leq Ch^p \tag{22}$$

where $\|\mathbf{e}_\mathbf{G}\|$ does not converge at all (i.e. with a rate h^0). Beyond P , the auxillary function is well behaved and hence

$$|\mathcal{F}_2(\mathbf{e})| \leq \sum_{\tau \in P'} \|\mathbf{e}_\tau\| \|\mathbf{e}_\mathbf{G}\| \leq Ch^{2p} \tag{23}$$

Thus, we have

$$|\mathcal{F}(\mathbf{e})| \leq Ch^p \tag{24}$$

Remark. Using definition E_2 will ensure that the elements with higher intensity of contribution to total error are refined. This guarantees accuracy of pointwise quantities in a neighborhood of the region of interest. This is crucial in first-ply failure computation as location of the point also changes with the mesh, till convergence is achieved.

Remark. When reentrant corners are present in the domain, or when the plate model locks, the global part of the error, $\mathcal{F}_2(\mathbf{e})$, may be dominant and the rate of convergence can be much lower. However, for the adaptive strategy we will adopt the ideal a priori estimates.

The goal of the adaptive process is to refine the given mesh selectively such that the total error is below the specified tolerance, i.e.

$$|\mathcal{F}(\mathbf{e})| \leq \eta |\mathcal{F}(\mathbf{u}_h)| \tag{25}$$

where $\mathcal{F}(\mathbf{u}_h)$ is the computed value of the desired quantity of interest; $|\mathcal{F}(\mathbf{e})|_{E_2}$ is obtained using definition E_2 for the error. Following [9], we will define $r_\tau = (h_d/h)$ as the ratio of the desired (h_d) to the actual mesh size (h) of the element τ . The desired mesh should have the least number of elements, of all possible meshes. Hence, following [9], we minimize

$$\sum_{\tau} \frac{1}{r_\tau^2}$$

subject to constraints (22) and (23). Thus, we define the new objective function (to be minimized) as,

$$J = \sum_{\tau} \frac{1}{r_\tau^2} + \lambda_1 \left(\sum_{\tau \in P} \chi_{d,\tau}^2 - \mathcal{F}_{d,1} \right) + \lambda_2 \left(\sum_{\tau \in P'} \chi_{d,\tau}^2 - \mathcal{F}_{d,2} \right) \tag{26}$$

where $\chi_{d,\tau} = |B(\hat{\mathbf{e}}_\tau, \hat{\mathbf{e}}_\mathbf{G})|$ is the desired contribution to the total error from element τ ; $\hat{\mathbf{e}}_\tau, \hat{\mathbf{e}}_\mathbf{G}$ are the desired errors in the element τ ; λ_1 and λ_2 are Lagrange multipliers; $\mathcal{F}_{d,1} = \eta_1 |\mathcal{F}(\mathbf{u}_h)|$ and $\mathcal{F}_{d,2} = \eta_2 |\mathcal{F}(\mathbf{u}_h)|$ are the desired errors in the region P and P' , respectively (here $\eta = \eta_1 + \eta_2$). Using (22) and (23) $\chi_{d,\tau}^2$ can be given in terms of the actual error $\chi_{a,\tau}^2$ (where $\chi_{a,\tau}^2 = |B(\mathbf{e}_\tau, \mathbf{e}_\mathbf{G})|$ in the element τ), as

For $\tau \in P$, $\chi_{d,\tau}^2 = r_\tau^p \chi_{a,\tau}^2$

For $\tau \in P'$, $\chi_{d,\tau}^2 = r_\tau^{2p} \chi_{a,\tau}^2$

Thus, (26) becomes

$$J = \sum_{\tau} \frac{1}{r_\tau^2} + \lambda_1 \left(\sum_{\tau \in P} r_\tau^p \chi_{a,\tau}^2 - \mathcal{F}_{d,1} \right) + \lambda_2 \sum_{\tau \in P'} \left(\sum_{\tau \in P'} r_\tau^{2p} \chi_{a,\tau}^2 - \mathcal{F}_{d,2} \right) \tag{27}$$

Minimizing J with respect to r_τ , λ_1 and λ_2 we get

For $\tau \in P$,

$$r_\tau = \frac{\mathcal{F}_{d,1}^{1/p}}{\left(\sum_{\tau \in P} \chi_{a,\tau}^{4/(p+2)} \right)^{1/p} \chi_{a,\tau}^{2/(p+2)}} \tag{28}$$

For $\tau \in P'$,

$$r_\tau = \frac{\mathcal{F}_{d,2}^{1/2p}}{\left(\sum_{\tau \in P'} \chi_{a,\tau}^{2/(p+1)} \right)^{1/2p} \chi_{a,\tau}^{1/(p+1)}} \tag{29}$$

Using the computed values of r_τ , the desired mesh sizes can be computed. The mesh can be locally refined several times based on the desired mesh size. This leads to a final adaptively refined mesh.

Remark. The partition of the contribution to the error from P and P' is based on the user. The final mesh depends on the choice of η_1 and η_2 . In order to keep both contributions of the same order, we choose $\eta_1 = \eta_2 = \eta/2$.

9. Numerical examples using one-shot focussed adaptivity

The adaptive procedure given above can be employed to selectively refine the initial mesh, in order to get the desired mesh (with error in the quantity of interest within the specified tolerance) in one shot. The computation has to be redone on the final mesh in order to obtain the quantity of interest. Below, we will demonstrate through numerical examples, for the thin plate, the effectiveness of this two-mesh solution process.

Let us consider the laminate configuration (thin plate) given previously. For this laminate, the $[0/90/90/0]$ and $[-45/45/45/-45]$ stacking sequences are taken. For the adaptive procedure we let the specified tolerance for the error in the quantity of interest be $\eta = 3\%$ error. For the initial mesh shown in Fig. 3, we let $\sigma_{xx,avg}^{(1)}$ and $\sigma_{yy,avg}^{(1)}$ (i.e. average stress components in the topmost layer) be the quantity of interest, for the element τ shaded gray. In Fig. 4 we show the final meshes obtained

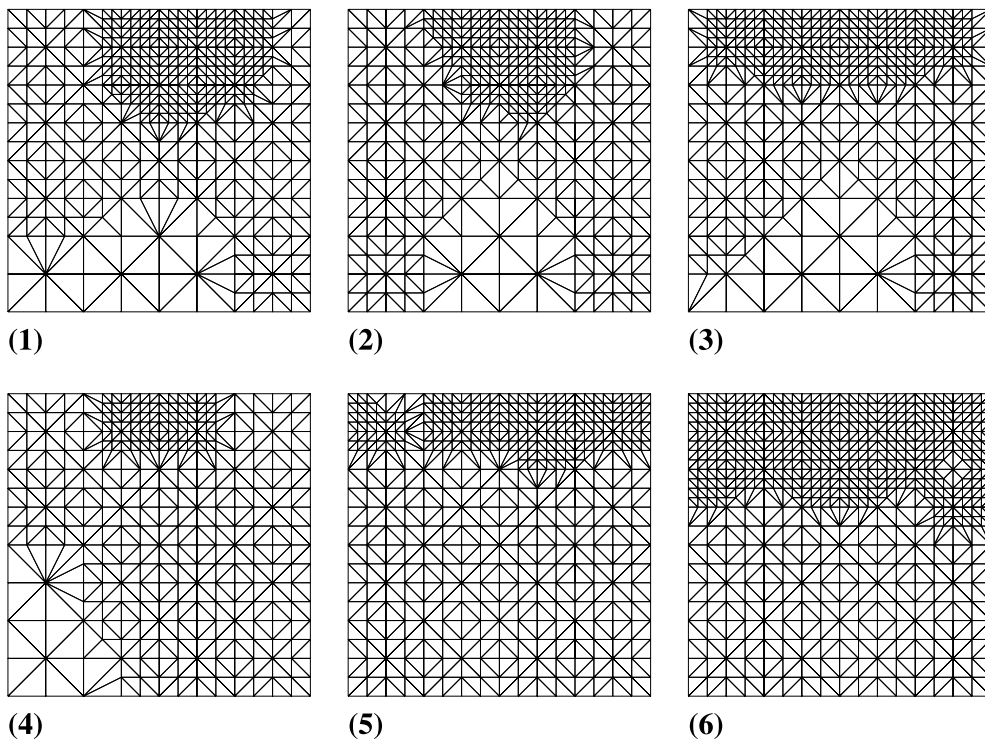


Fig. 4. One-shot adaptivity: definition E_2 for the error; the final meshes obtained for various choices of quantities of interest, boundary conditions and material orientations in each lamina (see Table 6 for the details).

Table 6
One-shot adaptivity for control of error in quantity of interest

Mesh	Laminate	Quantity	$ \mathcal{F}(\mathbf{e}) _{\text{init}}$	$ \mathcal{F}(\mathbf{e}) _{\text{fin}}$	$ \mathcal{F}(\mathbf{u}_h) $	η_{achieved}
1	[0/90/90/0] (SSSS)	$\sigma_{xx,\text{avg}}^{(1)}$	649.56	39.32	1558.36	0.025
2	[0/90/90/0] (SSSS)	$\sigma_{yy,\text{avg}}^{(1)}$	86.77	9.67	283.01	0.034
3	[0/90/90/0] (CFCF)	$\sigma_{xx,\text{avg}}^{(1)}$	18.03	0.75	57.66	0.013
4	[-45/45/45/-45] (SSSS)	$\sigma_{yy,\text{avg}}^{(1)}$	331.83	44.69	1933.11	0.023
5	[-45/45/45/-45] (CFCF)	$\sigma_{xx,\text{avg}}^{(1)}$	97.61	9.43	421.05	0.022
6	[-45/45/45/-45] (CFCF)	$\sigma_{yy,\text{avg}}^{(1)}$	613.09	31.31	834.63	0.037

Definition E_2 for the error in quantity; average stress in the topmost layer, in the element τ (shown shaded gray in Fig. 3); errors in the initial and final (adaptively refined) meshes.

by the adaptive process, using definition E_2 of the pointwise error estimator. In Table 6 the details of the material, quantity of interest, errors in the initial mesh ($|\mathcal{F}(\mathbf{e})|_{\text{init}}$) and the final mesh ($|\mathcal{F}(\mathbf{e})|_{\text{fin}}$), and the tolerance achieved (η_{achieved}) are reported for the meshes shown in Fig. 4. From the results we note that

- (1) The final meshes in all the cases correspond to an error within the specified tolerance ($0.013 \leq \eta_{\text{achieved}} \leq 0.037$).
- (2) The final mesh depends strongly on the quantity of interest, ply orientations and the boundary conditions.
- (3) The region of strong refinements is not restricted to the local region of interest only. It can spread to a larger part of the initial mesh, depending on the quantity of interest, boundary conditions and material orientation.
- (4) Almost the full mesh requires further refinements.

As a check, the quality of the error estimator (using definition E_2) for the final mesh 6, was obtained. The effectivity index was found to be $\kappa_{\mathcal{F}} = 0.70$. The true error in the quantity was 1.368 kPa, i.e. an error of less than 0.1%.

9.1. Effect of approximation order p

As observed above, for $p = 2$, the mesh is refined almost everywhere. This can be due to locking (which can be severe for thin plates). Use of higher order approximations removes the effect of locking. In order to

see this numerically, we let $p = 3$. In Table 7, we report the errors, and η_{achieved} .

The corresponding final meshes are shown in Fig. 5. From Fig. 5 and Table 7, we observe that

- (1) For $p = 3$, the target tolerance of $\eta = 0.03$ is achieved with a much coarser mesh.
- (2) The mesh refinement is localised mostly to the neighborhood of the region of interest.

It should be noted that for the domains and boundary conditions employed above, use of high p can lead to very accurate results everywhere. For $p = 3$, and the problems considered, the locking effect is negligible. It should further be noted that the boundary-layer from boundaries not adjacent to the region of interest does not effect the local quantity of interest significantly, for the class of problems considered here.

Remark. For some of the cases in Tables 6 and 7, the value of η_{achieved} is much smaller than the desired value of $\eta = 0.03$ (for example mesh 3 of Table 6 and mesh 2 of Table 7). This is because the η for the initial mesh was close to the threshold. The desired mesh sizes for these cases would be close to the original one (but smaller). Thus the refinement process would refine all the elements with a smaller (desired) mesh size, leading to an “over-kill”, or a much more accurate solution than desired.

9.2. Adaptivity for a domain with a cut-out

Generally composite panels, employed in practical applications, have cut-outs (for window openings,

Table 7
Effect of order of approximation

Mesh	Laminate	Quantity	$ \mathcal{F}(\mathbf{e}) _{\text{in}}$	$ \mathcal{F}(\mathbf{e}) _{\text{fin}}$	η_{achieved}	No. of DOFs
1	[0/90/90/0] (SSSS)	$\sigma_{xx,\text{avg}}^{(1)}$	24.4	24.4	0.016	625×8 (1520×8)
2	[0/90/90/0] (SSSS)	$\sigma_{yy,\text{avg}}^{(1)}$	10.2	0.8	0.003	967×8 (1429×8)
3	[-45/45/45/-45] (CFCF)	$\sigma_{xx,\text{avg}}^{(1)}$	70.9	20.0	0.024	1330×8 (2264×8)

Definition E_2 for error in quantity; average stress in the topmost layer, in the element τ (shown shaded gray in Fig. 3); errors in the initial and final (adaptively refined) meshes for $p = 3$. The quantities in parentheses in the last column correspond to the final mesh for $p = 2$.

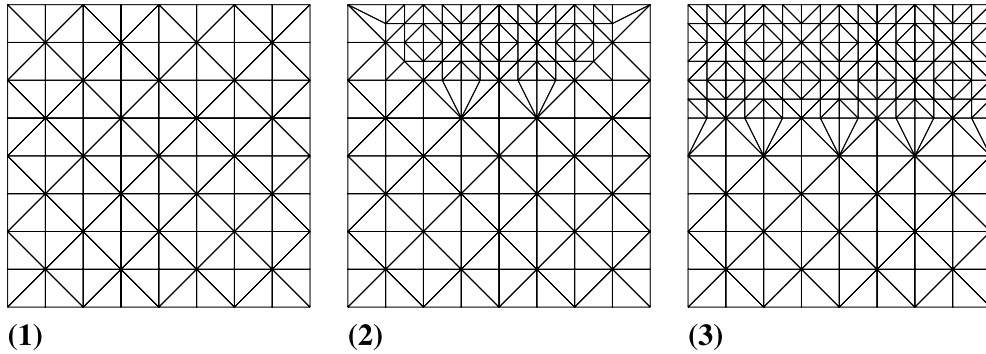


Fig. 5. One-shot adaptivity: definition E_2 for error in quantity; average stress in the topmost layer, in the element τ (shown shaded gray in Fig. 3); the final meshes obtained for various choices of quantities of interest, boundary conditions and material orientations in each lamina (see Table 7 for the details); $p = 3$.

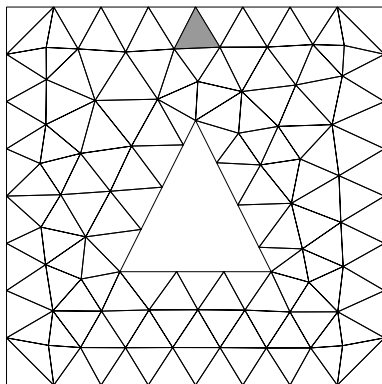


Fig. 6. One-shot adaptivity: the initial mesh for domain with cut-out; element of interest τ shown shaded gray.

inspection bays, or for weight saving). In order to study the effect of cut-outs on the adaptive process, we consider the domain of Fig. 6, with a triangular cut-out. For this domain, the initial mesh is as shown in Fig. 6. As detailed in Table 8, the final meshes were obtained for various combinations of quantities, boundary conditions and ply orientations. Results for both $p = 2$ and 3 have been reported, for the element τ shown shaded gray in Fig. 6 for the topmost layer (i.e. $l = 1$). From Table 8 we note that

- (1) For $p = 2$ the desired tolerance is achieved with significantly higher number of degrees of freedom, as compared to $p = 3$.
- (2) Even for $p = 3$, the given initial mesh was not sufficient, leading to a significantly refined final mesh.
- (3) The final meshes are very sensitive to the quantity of interest, ply orientations, and boundary conditions.
- (4) Refinement near the corners of the cut-out depends on the quantity of interest, boundary condition and the ply orientations. Refinements near the cut-out can be significant even for $p = 3$. This is because of stress concentrations arising at the corners of the cut-outs.
- (5) The desired levels of refinement is not the same at each of the corners of the cut-out. The desired level depends on the quantity, material orientation and boundary conditions.
- (6) The value of η_{achieved} is generally higher than 0.03.

The higher final tolerance is due to the fact that the corners in the cut-out cause a suboptimal rate of convergence of the finite element solution. Thus, the desired mesh sizes, obtained using the optimal rate of convergence, are higher than the true one. However, a further iteration of the refinement process will lead to the de-

Table 8
One-shot adaptivity for a domain with a cut-out

Mesh	p	Laminae	Quantity	$ \mathcal{F}(\mathbf{e}) _{\text{in}}$	$ \mathcal{F}(\mathbf{e}) _{\text{fin}}$	η_{achieved}	No. of DOFs
1	2	[0/90/90/0] (SSSS)	$\sigma_{yy,\text{avg}}^{(1)}$	85.4	2.46	0.021	4096×8
2	2	[0/90/90/0] (CCCC)	$\sigma_{xx,\text{avg}}^{(1)}$	94.0	5.7	0.041	2673×8
3	2	[-45/45/45/-45] (CFCF)	$\sigma_{yy,\text{avg}}^{(1)}$	126.1	15.9	0.031	1777×8
4	3	[0/90/90/0] (SSSS)	$\sigma_{yy,\text{avg}}^{(1)}$	31.7	4.7	0.041	2088×8
5	3	[0/90/90/0] (CCCC)	$\sigma_{xx,\text{avg}}^{(1)}$	29.0	6.1	0.045	1821×8
6	3	[-45/45/45/-45] (CFCF)	$\sigma_{yy,\text{avg}}^{(1)}$	18.3	7.6	0.015	1422×8

Effect of order of approximation; definition E_2 for error in quantity; average stress in the topmost layer, in the element τ (shown shaded gray in Fig. 6); errors in the initial and final (adaptively refined) meshes for $p = 2, 3$.

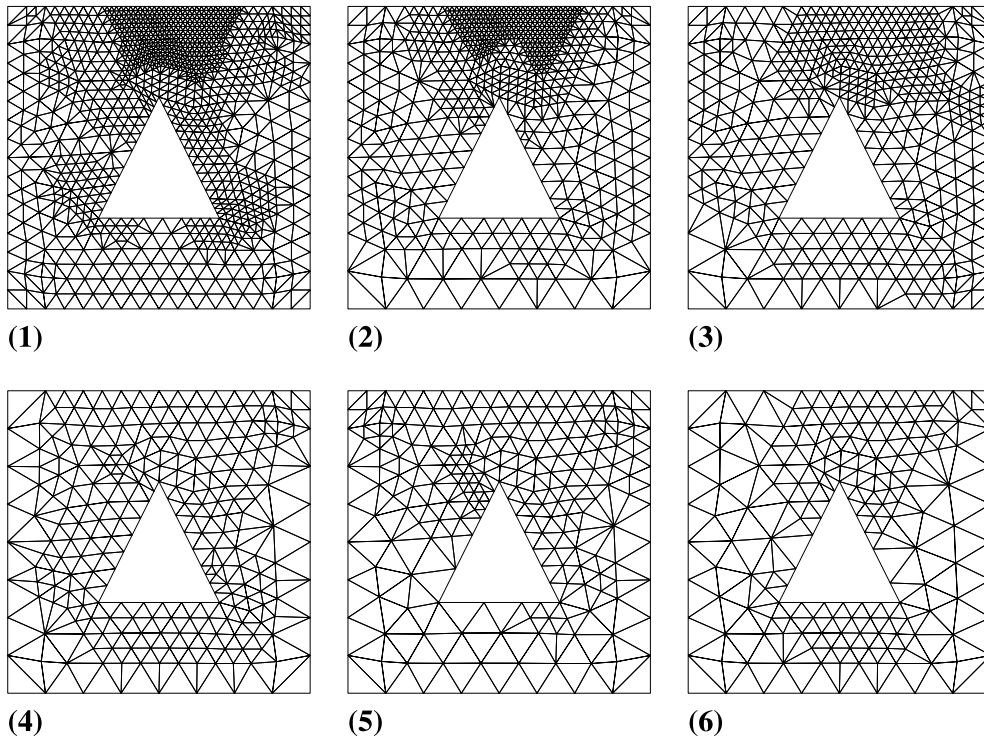


Fig. 7. One-shot adaptivity: definition E_2 for error in quantity; average stress in topmost layer for element shown shaded gray in Fig. 6; the final meshes obtained for various choices of quantities of interest, boundary conditions and material orientations in each lamina (see Table 8 for the details). Meshes 1, 2 and 3 correspond to $p = 2$; the corresponding final meshes for $p = 3$ are given by meshes 4, 5 and 6 respectively.

sired mesh. Note that, inspite of the restrictive assumption on the rate of convergence, the mesh obtained is always close to the desired one. Hence, the one-shot adaptive refinement procedure is very effective (Fig. 7).

10. Conclusions

The goal of this study was to develop an adaptive finite element procedure, based on a posteriori error estimation and adaptive refinement of the mesh, for accurate computations of critical local quantities of interest for laminated composite plates. From the results, we conclude that

- (1) The estimation of the error in the local quantity of interest requires computation of the solution corresponding to an auxiliary problem. This leads to an additional load-vector for the standard finite element computations.
- (2) The estimates of the error in the local quantity can be obtained using the standard a posteriori error estimators available in the literature.
- (3) Employing a L_2 -recovery based error estimator, quick and reliable estimates of the error in the quantity of interest can be obtained.
- (4) The adaptive algorithm employs the partitioning of the contribution to the total error, in the quantity of interest, into local and far-field components. The local contribution converges at the rate of h^p and the far-field (or pollution) part converges at the rate of h^{2p} (in the absence of locking and re-entrant corners).
- (5) The final (optimal) meshes obtained by employing the a priori convergence rates for the local and far-field parts of the error were close to the desired ones, i.e. the total error in the quantity of interest was close to the specified tolerance, even for domains with cut-outs.
- (6) The meshes obtained depend strongly on the boundary conditions, material orientation and the quantity of interest.
- (7) The desired meshes require strong refinements in the vicinity of the local region of interest, and significant refinements elsewhere for $p = 2$. The strong refinements can spread to a large part of the mesh, depending on various factors. This leads to the proper

global–local approach for accurate computation of critical local quantities of interest.

- (8) Generally, the boundary layer effect was not significant for the local quantity of interest, for the class of problems studied here. The adaptive procedure is capable of resolving these effects through proper refinement of the desired boundaries.
- (9) For higher p (i.e. $p = 3$), the desired tolerance can be achieved with a coarser mesh, as compared to that for $p = 2$.
- (10) In the presence of cut-outs, refinement near the corners of the cut-out are required, especially for the corners closer to the region of interest. However, the level of refinement is strongly influenced by the choice of the quantity of interest, material, boundary conditions and approximation order.

References

- [1] Abrate S. Optimal design of laminated plates and shells. *Compos Struct* 1994;29:269–86.
- [2] Actis RL, Szabo BA, Schwab C. Hierarchic models for laminated plates and shells. *Comput Meth Appl Mech Engng* 1999;172:79–107.
- [3] Kapania RK, Raciti S. Recent advances in analysis of laminated beams and plates. Part I: shear effects and buckling. *AIAA J* 1989;27(7):923–34.
- [4] Mohite PM, Upadhyay CS. Local quality of smoothening based a-posteriori error estimators for laminated plates under transverse loading. *Comput Struct* 2002;80:1477–88.
- [5] Babuska I, Strouboulis T, Mathur A, Upadhyay CS. Pollution error in the h version of the finite element method and the local quality of a-posteriori error estimators. *Finite Elem Anal Des* 1994;17:273–321.
- [6] Babuska I, Strouboulis T, Upadhyay CS, Gangaraj SK. A posteriori estimation and adaptive control of the pollution error in the h version of the finite element method. *Int J Numer Meth Engng* 1995;38:4207–35.
- [7] Babuska I, Strouboulis T, Upadhyay CS. A model study of the quality of a posteriori error estimators for linear elliptic problems. Error estimation in the interior of patchwise uniform grids of triangles. *Comput Meth Appl Mech Engng* 1994;114:307–78.
- [8] Wahlbin LB. Local behavior in finite element methods. In: Ciarlet PG, Lions JL, editors. *Handbook of numerical analysis*, vol. II. North Holland; 1991. p. 357–521.
- [9] Ladeveze P, Pelle JP, Rougeot PH. Error estimation and mesh optimization for classical finite elements. *Engng Comput* 1991;8:69–80.
- [10] Zienkiewicz OC, Zhu JZ. A simple error estimator and the adaptive procedure for practical engineering analysis. *Int J Numer Meth Engng* 1987;24:337–57.
- [11] Verfurth R. *A review of a-posteriori error estimation and adaptive mesh-refinement*. New York: Wiley Tuebner; 1996.